GEOPERSIA

Accepted Manuscript

Identification and Estimation of Groundwater Recharge Sources through Hydrochemical Analysis and Stable Environmental Isotopes in Evan Plain, Khuzestan, Iran

Zahra Chaghazardi, Seyed Yahya Mirzaee, Manouchehr Chitsazan, Farshad Alijani

Identification and Estimation of Groundwater Recharge Sources through Hydrochemical Analysis and Stable Environmental Isotopes in Evan Plain, Khuzestan, Iran

Zahra Chaghazardi [1] , **Seyed Yahya Mirzaee** [1, *] , **Manouchehr Chitsazan** [1] , **Farshad Alijani** [2]

[1] Faculty of Geosciences, Shahid Chamran University of Ahvaz, Iran
[2] Faculty of Geosciences, Shahid Beheshti University of Tehran, Iran

Abstract
Identifying the inflows and outflows of plains experiencing groundwater level fluctuations is a critical aspect of water resource management, environmental decision-making, and agricultural planning. Identifying these recharge sources and quantifying their contributions are essential for sustainable aquifer management due to the rising water table in the Evan Plain in southwestern Iran. This study used hydrogeological, hydrochemical, statistical, and isotopic methods to identify and evaluate the recharge sources of the plain. Groundwater sampling was conducted during the dry and wet seasons (August 2022) and the wet seasons (May 2023). The results of hydrogeological assessments, hydrochemical analyses, hierarchical cluster analysis (HCA), and isotopic investigations reveal that the groundwater of the Evan Plain is mainly affected by two recharge sources. The Karkheh River, contributing an average of 30%, serves as the main recharge source in the northern and northeastern parts of the plain. Furthermore, The groundwater inflow from the Abbas Plain contributes an average of 32% to the aquifer recharge, predominantly affecting the plain's central, southeastern, and southwestern areas. These findings provide valuable insights for effective aquifer management and future regional water resource planning.

Introduction

In the arid climate of southwestern Iran, groundwater serves as a critical resource for agricultural and domestic needs, particularly in regions like the Evan Plain where surface water supplies are limited (Kumar, 2012). The global extraction of groundwater has reached approximately 1,500 km^3 per year (Parlov, Nakić et al., 2012), which exceeds the natural recharge rate of groundwater (Nakić, Ružičić, et al., 2013). Moreover, many alluvial aquifers face challenges due to groundwater depletion, which has become a global concern (Wada, van Beek et al., 2012; Gleeson, Befus et al., 2016). Most studies in groundwater resource management have focused on groundwater reservoir deficits and excessive depletion of these resources. However, since the rise of groundwater levels is a relatively rare global occurrence, few studies have been on this issue. In other words, rising groundwater levels reduce groundwater depth relative to the surface, increasing the risk of groundwater contamination and other related problems. All these issues underscore the need for precise research and identification of recharge sources and the calculation of groundwater recharge to ensure the

* Corresponding author e-mail: Yahya2010@yahoo.com

sustainable management of groundwater resources. In this context, several studies have been conducted by researchers (Gat, 2010; Wang, Li et al., 2015; Bouimouass, Fakir et al., 2020; Dar, Jeelani et al., 2021; Huang, Ping et al., 2021; Balagizi, Kasereka et al., 2022; Xu, Li et al., 2023; Cocca, Lasagna et al., 2024).

(Schwarz, Barth et al., 2009), Evaluated the mixing between different parts of groundwater reservoirs in one of Germany's largest and most well-known karst regions by comparing the isotopic composition of precipitation and groundwater discharge. (Marques, Graça et al., 2013), Groundwater recharge and local and regional flow paths in a limestone system in central Portugal were examined using isotopic tracers. (Fu, Li et al., 2018), Studied the origin of groundwater and the evolution of hydrochemistry in the middle basin of the Kuye River in China using hydrochemical and isotopic studies. (Joshi, Rai et al., 2018), conducted a study tracing the recharge sources of groundwater in the alluvial aquifer in northwestern India using isotopes (O18, H2, and H3). The results indicated that local rainfall was the main source of groundwater recharge, although depleted O18 and H2 in certain locations suggested recharge from irrigation canals and return flow from irrigation water.

(Parlov, Kovač et al., 2019), The interactions between precipitation, surface water, and groundwater in the Zagreb aquifer system were explored using stable isotopes in water. They calculated the contribution of groundwater, precipitation, and surface water as recharge sources in each sampled well using two- and three-component mixing models. Karlović et al., 2021; Marković et al., 2021) Investigated groundwater recharge rates in the Upper Awash Basin in Ethiopia under various model complexities and objective functions. Their study used water temperature monitoring, chloride content, and stable isotopes as inputs for a mixing model to quantify the contribution of each recharge source.

(Al-Ruwaili et al., 2023), This study used stable isotopes ($\delta^{18}O$ and δ^2H), hydrochemical analyses, Netpath geochemical modeling, and principal component analysis (PCA) to identify groundwater recharge sources. Findings show that local rainfall is the main recharge source, with evaporation and silicate weathering playing significant roles.

(Putra et al., 2023), Stable isotopes and hydrochemical data indicated that effective recharge zones are located at specific elevations, and silicate weathering is a major influencing process.

(Moussa et al., 2024), This study based on stable isotope and chemical data revealed that local precipitation and interaction with surface water are the main groundwater recharge sources.

(Nadiri, 2016), examined the hydrogeochemistry and hydrogeology of the Herzandat Plain aquifer using statistical and graphical methods. The results showed that, according to the Piper and Stiff diagrams, groundwater sources have two and six distinct origins, respectively. The Durov diagram indicated two main hydrogeochemical processes in the aquifer, while hierarchical cluster analysis (HCA) revealed five water types in the groundwater samples, as cluster analysis can handle a larger dataset than graphical methods. Previous studies, such as Mohammadzadeh and Eskandari (2018), have successfully applied hydrogeochemical and isotopic techniques to assess water resources in neighboring areas, like Paveh and Javanrud in Kermanshah Province. Building on this foundation, the present study applies similar methodologies to investigate groundwater recharge in the Evan Plain.

This study aims to identify and evaluate the recharge sources of the Evan Plain using an integrated approach that combines hydrochemical, isotopic, and statistical analyses, in order to quantify their contributions to the aquifer system. Unlike previous studies in the region, which primarily relied on individual methods such as hydrochemical analyses, this research provides a more comprehensive understanding of groundwater recharge dynamics by capturing both spatial and temporal variability. The recent rise in groundwater levels within the plain has resulted in considerable challenges, including the risk of waterlogging, soil salinization, and adverse effects on agricultural productivity and water quality. Understanding the nature and

relative contributions of different recharge sources is therefore essential for developing sustainable groundwater management strategies. The findings from this study offer a new perspective for regions influenced by multiple recharge sources and will serve as a scientific foundation for informed decision-making, long-term water resource planning, and the prevention of further environmental degradation.

Materials and Methods

Study Area

The Evan Plain, with an area of 195 km^2, is located in the southernmost mountainous part of the Karkheh River basin, approximately between the longitudes of 47°59′ to 48°9′ E and latitudes of 32°14′30″ to 32°24′30″ N. The plain is triangular (Fig. 1), with its eastern side bordering the Karkheh River, the southwestern side adjacent to the Dosalag Plain, the northwestern side meeting the Karkheh Dam, and its western tip connecting to the surface outflow of the Abbas Plain (Kalantari, Rahimi et al., 2012).

The study area is part of the folded Zagros structural-sedimentary basin. From a stratigraphic perspective, the most important sedimentary units in the region are associated with the Bakhtiari Formation and the Lahbari Member. These formations are the primary factors influencing the quantity and quality of groundwater in the region. The lithology of the Bakhtiari Formation mainly consists of conglomerates with calcareous cement, though sandy and silty cement can occasionally be observed. In this region, the Bakhtiari Formation has limited strength, and over time, due to water erosion, it has lost its carbonate cement, filling the synclines with its eroded sediments. The lithology of the Lahbari Member includes marl, siltstone, and shale. The Evan Plain syncline, part of the larger Dezful Plain syncline, is filled with alluvial sediments resulting from the erosion of surrounding formations. In the Evan Plain, the grain size of sediments decreases from the northern and northwestern parts toward the south and southeast. The coarse-grained particles are primarily derived from the disintegration of the Bakhtiari Formation, while the fine-grained sediments result from the erosion of the Lahbari Member and alluvial deposits.
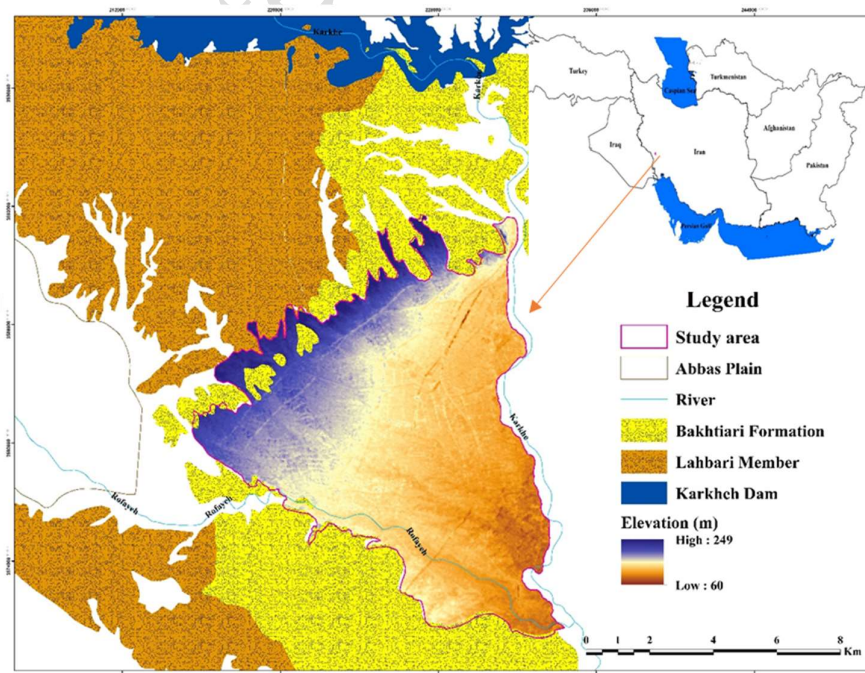

Figure 1. Location of the study area

The erosive agents include stream channels, the large Karkheh River, and the Rofaiyeh River. These streams deposit coarse-grained sediments upon entering the plain, while finer sediments are transported and deposited further along their course, causing the grain size of the sediments in the northern and northwestern parts of the Evan Plain to be coarse, and becoming finer toward the southern and southeastern parts.

Vertically, the grain size begins as fine to medium in the upper layers, becomes coarser, and eventually transitions back to fine-grained sediments, culminating in a compact clay layer. The aquifer in the Evan Plain has formed in this intermediate coarser-grained layer. The Karkheh River is the only permanent river passing through the Evan Plain and plays a significant role in meeting the region's water needs. This river's high quality of water makes it widely utilized for various purposes, particularly in providing irrigation water for a large portion of the plain's agricultural needs.

Sampling and analysis

To thoroughly investigate the recharge sources of the Evan Plain aquifer, samples were collected from groundwater sources (EV, AB), rainfall (P), the irrigation and drainage network (Ir), the Karkheh Dam (D), and the Karkheh River (RK) during two periods: in August 2022 (dry season) and May 2023 (wet season). Sampling included major ions (during the dry and wet seasons) and stable isotope samples (during the dry season), as illustrated in Figure 2. The chemical analysis of major anions and cations (Ca^{2+}, Mg^{2+}, Na^+, K^+, Cl^-, SO_4^{2-}, HCO_3^-, Br^-, NO_3^-) was conducted in the laboratory of the Khuzestan Water and Power Authority (Tables 1 and 2). In this laboratory, calcium, magnesium, chloride, carbonate, and bicarbonate were measured using titration methods; sodium and potassium using flame photometry; and sulfate and nitrate using a spectrophotometer (UV-Vis model DR2800) and the absorbance of bromine was measured using spectrophotometry at 420nm with a UV-Vis spectrophotometer. This method was selected due to its high sensitivity and accuracy for detecting trace amounts of bromine.
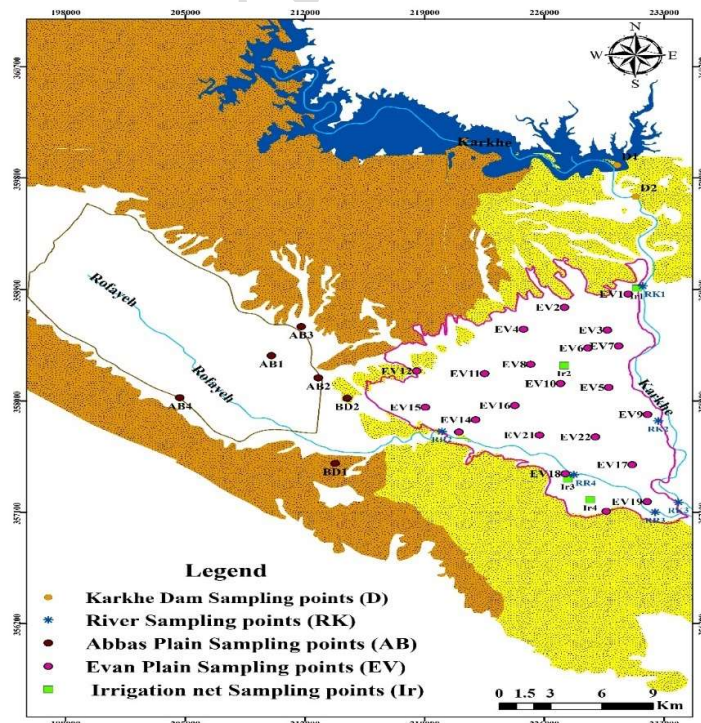

Figure 2. Location of sampling points

A digital conductivity meter was used to measure the pH and electrical conductivity (EC) on-site. Sampling locations were strategically selected based on hydrological, geological, and land-use patterns to capture the spatial variability of recharge characteristics across the study area. Particular attention was given to areas with distinct lithological formations and aquifer types to ensure a representative and comprehensive coverage. Moreover, sites with higher recharge potential—identified through preliminary hydrogeological surveys—were prioritized. This sampling strategy enhances the reliability of the results and ensures that they reflect the behavior of the broader groundwater system in the Evan Plain.

Initially, the total concentration of anions and cations in the sampled wells was measured in milliequivalents per liter, and the percentage error was calculated. The error margin was determined to be 1.3%, below the acceptable limit of 5%, making this margin of error satisfactory. For statistical methods, the Kaiser method was used to standardize the data, which confirmed the normal distribution of the data (Chitsazan et al., 2018).

Table 1. Hydrochemical and isotopic data (dry season)

Names of sampling points	Ca (Meq/l)	Mg (Meq/l)	Na (Meq/l)	K (Meq/l)	Hco3 (Meq/l)	SO4 (Meq/l)	Cl (Meq/l)	Br (Meq/l)	No3 (Mg/l)	$\delta^{18}O$ (%)	$\delta\,^2H$ (%)
EV1	3.81	6.39	4.32	0.06	2.62	6.83	6.4	0.16	3.84	-3.37	-18.68
EV2	1.56	5.26	1.85	0.05	2.4	3.28	3.37	0.13	42.45	-2.58	-10.51
EV3	5.05	5.67	4.11	0.06	3.35	5.89	5.86	0.16	21.95	-3.24	-20.43
EV4	2.09	3.34	2.06	0.04	2.15	2.99	2.53	0.12	34.93	-1.37	-13.46
EV5	12.65	9.9	12.43	0.14	4.7	17.38	13.64	0.77	26.98	-2.91	-21.12
EV6	12.77	10.89	6.71	0.08	3.15	11.38	5.57	0.27	22.33	-2.48	-17.97
EV7	6.64	7.49	7.09	0.11	4.7	10.1	7.31	0.22	25.04	-2.79	-21.07
EV8	6.55	10.56	5.17	0.07	2.7	10.92	5.45	0.28	35.63	-1.64	-18.58
EV9	5.93	5.64	5.44	0.08	3.51	6.47	7.15	0.23	26.35	-2.3	-25.23
EV10	13.89	10.17	9.76	0.09	2.54	12.96	5.49	0.41	17.06	-2.09	-19.29
EV11	7.54	8.55	6.3	0.06	1.9	10.05	5.32	0.24	29.30	-2.16	-19.29
EV12	8.4	8.72	4.05	0.03	2	10.92	5.35	0.12	21.24	-2.65	-12.21
EV13	11.86	12.9	16.2	0.11	2.75	26.9	13.6	0.61	21.12	-2.92	-10.92
EV14	16.23	17.76	15.47	0.09	2.08	34.28	15.04	0.74	51.60	-2.45	-4.95
EV15	9.01	10.66	17.44	0.08	2.9	27.08	8.44	0.44	33.06	-2.39	-10.09
EV16	21.07	14.42	13.88	0.12	2.74	35.46	11.39	0.71	30.36	-3.29	-13.81
EV17	13.63	10.61	13.01	0.08	3.55	24.18	9.86	0.51	23.14	-2.73	-13.67
EV18	16.74	14.38	10.21	0.08	3.1	33.35	6.2	0.43	28.07	-3.18	-13.15
EV19	3.25	3.57	4.18	0.05	2.94	5.25	3.12	0.14	12.49	-4.37	-20.43
EV20	13.32	14.28	11.19	0.08	2.56	29.34	8.25	0.57	51.27	-2.41	-11.01
EV21	20.9	20.16	15.64	0.15	2.67	41.15	13.75	0.55	50.51	-3.14	-12.32
EV22	26.15	17.66	26.49	0.18	2.97	48.35	17.94	1.02	36.26	-3.11	-8.8
BD1	6.98	4.82	14.7	0.06	2.38	12.69	8.33	0.32	16.32	-3.23	-9.14
BD2	11.92	11.45	21.78	0.1	2.05	28.4	14.73	0.59	18.04	-3.25	-9.76
AB1	5.43	10.14	4.24	0.07	1.74	16.76	3.47	0.21	37.33	-2.03	-9.53
AB2	2.28	2.47	3.66	0.04	2.1	8.89	3.54	0.09	16.57	-2.65	-11.74
AB3	0.99	1.16	2.03	0.03	1.98	6.37	2.6	< 0.06	15.23	-2.95	-9.27
AB4	9.86	16.78	7.54	0.07	2.09	29.63	5.91	0.27	25.99	-3.03	-15.31
RK1	3.58	6.59	9.59	0.11	2.6	8.79	10.11	0.26	2.04	-3.69	17.02
RK2	2.7	5	5.78	0.06	3.15	5.41	7.08	0.14	2.13	-4.2	-21.79
RK3	3.5	4.66	4.91	0.08	3.84	5.39	6.85	0.14	2.63	-4.73	-25.56
Ir1	3.52	6.57	9.55	0.09	2.7	11.73	10.07	0.26	2.02	-3.63	-16.56
Ir2	3.49	6.59	9.58	0.1	2.65	8.73	10.08	0.26	2.32	-3.69	-16.86
Ir3	3.58	6.53	9.79	0.09	2.67	8.33	10.01	0.22	1.40	-3.76	-18.23
Ir4	3.48	6.39	9.5	0.08	2.84	8.19	9.71	0.22	1.35	-3.41	-16.78
D1	3.42	6.34	11.27	0.09	2.37	8.34	11.87	0.22	1.21	-3.24	-9.04
D2	3.21	6.72	9.78	0.12	2.51	8.11	10.43	0.21	0.33	-3.87	-15.12
Standard Deviation	6.2	4.6	5.6	0.6	0.7	11.9	3.9	0.2	15.2	0.7	7.3

Table 2. Hydrochemical data (wet season)

Names of sampling points	Ca (Meq/l)	Mg (Meq/l)	Na (Meq/l)	K (Meq/l)	Hco3 (Meq/l)	SO4 (Meq/l)	Cl (Meq/l)	Br (Mq/l)	No3 (Mg/l)
EV1	10.29	4.49	5.63	0.07	2.47	8.18	9.79	0.25	7.69
EV2	7.29	1.4	1.71	0.06	2.17	3.61	3.78	0.14	49.25
EV3	7.45	4.34	3.73	0.06	2.64	5.74	6.27	0.2	26.98
EV4	4.47	1.8	2.21	0.04	1.67	3.3	2.78	0.13	36.73
EV5	13.82	12.11	13.06	0.12	4.31	19.12	15.16	0.83	35.48
EV6	15.3	12.27	7.25	0.09	2.67	13.71	5.92	0.27	27.61
EV7	10.3	6.26	7.26	0.12	4.29	10.71	8.05	0.22	24.78
EV8	15.06	6.48	5.85	0.1	2.27	11.41	7.3	0.29	37.89
EV9	8.15	5.85	5.86	0.11	3.25	7.41	8.35	0.31	31.55
EV10	14.92	14.37	11.57	0.09	2.29	16.66	6.67	0.5	28.37
EV11	13.38	7.9	6.88	0.1	1.84	19.14	6.44	0.32	41.93
EV12	9.71	7.96	3.97	0.05	1.85	10.75	5.45	0.16	25.31
EV13	18.12	11.7	16.29	0.13	2.45	32.13	11.68	0.6	38.64
EV14	25.07	15.37	14.61	0.14	1.63	35.46	17.93	0.95	74.94
EV15	15	9.19	18.69	0.1	2.49	30.09	9.93	0.56	44.00
EV16	20.56	20.15	15.18	0.18	2.45	39.28	13.56	0.96	45.97
EV17	15.98	13.97	14.4	0.1	3.32	28.78	11.77	0.47	34.07
EV18	21.18	16.32	11.45	0.11	3.12	38.51	7.34	0.59	30.00
EV19	4.92	3.36	4.52	0.07	2.8	5.6	3.48	0.17	17.18
EV20	19.42	13.39	13.71	0.11	2.34	35.63	7.63	0.6	59.81
EV21	28.99	20.48	17.63	0.18	2.53	47.7	16.4	0.75	67.98
EV22	26.34	27.11	30.44	0.23	2.81	58.34	22.05	1.42	63.03
BD1	12.81	10.45	15.22	0.08	1.21	28.89	8.48	0.45	33.66
BD2	15.32	11.18	22.09	0.08	1.88	31.09	16.11	0.76	30.15
AB1	26.34	15.92	18.91	0.15	1.85	38.19	21.33	1.01	36.72
AB2	3.45	2.27	3.83	0.04	1.83	9.43	3.79	0.12	18.99
AB3	1.75	0.99	1.57	0.02	1.66	8.44	2.48	< 0.06	18.47
AB4	22.01	13.42	11.23	0.15	1.92	39.3	4.49	0.58	73.81
RK1	11.24	3.72	8.77	0.11	2.35	10.95	10.29	0.24	10.58
RK2	3.51	1.26	1.21	0.04	2.65	1.62	1.16	< 0.06	6.69
RK3	4.76	2.37	6.34	0.05	2.73	5.85	6.28	< 0.06	5.54
Ir1	11.21	3.65	8.54	0.11	2.39	10.86	10	0.24	11.04
Ir2	11.05	3.63	8.51	0.13	2.36	10.71	9.99	0.24	10.69
Ir3	11.11	3.7	8.37	0.12	2.35	10.65	9.83	0.24	10.54
Ir4	11.19	3.7	8.73	0.13	2.24	11.01	10.2	0.23	10.75
D1	10.89	3.73	7.58	0.12	2.39	10.19	9.24	0.23	10.78
D2	8.86	2.86	6.17	0.1	2.08	10.04	6.6	0.18	10.21
Standard Deviation	6.9	6.4	6.4	0	0.6	14.5	5	0.3	19.2

In the next stage, the suitability of the data for statistical analysis was evaluated. The Kaiser-Mayer-Olkin (KMO) index and the Athlete Test were used for this purpose. The KMO index for the Evan Plain data was estimated to range between 0 and 1, with the KMO values exceeding 0.58, indicating that the data were appropriate for statistical analysis (Mirzaee et al., 2019). According to Bartlett's test, statistical analysis is considered valid when the P-value is less than the alpha level. The P-value represents the error probability; the alpha level is typically set at 0.05. Based on the calculations, the P-value was <0.0001, below the 0.05 error threshold, thus making statistical analysis possible.

Water samples were filtered through 0.45-micron filters for stable isotope analysis before being collected in sterile 50 mL polyethylene bottles. To prevent contamination and isotopic

fractionation, stringent protocols were followed during sample collection, storage, and transport. All sampling equipment was thoroughly cleaned and rinsed with distilled water before use. Samples were collected in pre-cleaned, airtight glass bottles to minimize air exchange and evaporation. To ensure preservation, the samples were stored in refrigerated conditions at 4°C during transport to the laboratory. and then sent to the Misbah Energy Laboratory. The equipment used for measuring stable isotopes δ^2H and $\delta^{18}O$ in this laboratory was a high-precision laser spectroscopy device (LGR), and the testing method followed the MEL-WI-12 protocol, calibrated with IAEA standards (Table 1 and 2).

Flow direction maps, groundwater depth maps, Piper diagrams, hierarchical cluster analysis (HCA), and isotope methods were used to assess Evan Plain's recharge sources and calculate each source's contribution. To achieve the objectives of this study, the software MATLAB, Excel, Aq.QA, Surfer, XLSTAT, and ArcGIS 10.5 were employed.

Hierarchical Cluster Analysis (HCA)

Cluster analysis is used to determine relative similarity, which reflects the homogeneity of measured parameter characteristics. This statistical method is widely applied in the analysis of multivariate data, including investigating relationships between variables, organizing samples into meaningful structures, and reducing the composition of groundwater in a region into a limited number of clusters. Cluster analysis groups a set of variables into homogeneous clusters, resulting in both internal (within-cluster) and external (between-cluster) homogeneity (Shrestha and Kazama, 2007). Various methods exist for classifying data, but statistical clustering is one of earth sciences's most important and widely used techniques (Davis and Sampson, 1986; Belkhiri et al., 2011). By using statistical clustering, samples can be categorized into distinct groups that are geologically and statistically significant (Steinhorst and Williams, 1985).

Isotopic Methods

Modern and precise methods in geochemical and hydrogeological studies include the use of stable isotopes, such as $\delta^{18}O$ and δ^2H. Stable isotopes δ^2H and $\delta^{18}O$ in water are widely used as natural tracers to understand hydrogeological processes such as precipitation, groundwater recharge, and the relationship between surface and groundwater, as well as a watershed's hydrology. The isotopic composition of $\delta^{18}O$ and δ^2H in water closely mirrors their composition in atmospheric water, meaning that it records the initial formation conditions of atmospheric water and can serve as a stable natural tracer. Based on this, after collecting information on atmospheric water and stable isotopes $\delta^{18}O$ and δ^2H in groundwater and analyzing the hydrogeological structure and groundwater flow in the target area, the groundwater recharge conditions and various recharge sources can be. Also, studying stable isotopes $\delta^{18}O$ and δ^2H can help identify different recharge areas (Clark and Fritz, 1997). In this study, through sampling and analyzing the stable isotopes $\delta^{18}O$ and δ^2H from rainwater, groundwater from the Evan (EV) and Abbas plains (AB), Karkheh Reservoir Dam (D) the irrigation and drainage network (Ir), and the Karkheh River (RK), the atmospheric water line equation for the study area was established, and the recharge sources for the Evan Plain were identified.

The Isotopic Line of Atmospheric Water and the Origin of Precipitation

One of the most notable relationships observed in water geochemistry is the near-linear correlation between $\delta^{18}O$ and δ^2H in atmospheric waters(Clark and Fritz, 1997). In 1961, Craig was the first to publish the relationship between $\delta^{18}O$ and δ^2H in freshwater on a global scale, known as the Global Meteoric Water Line (GMWL). The equation for the GMWL under

equilibrium conditions at a temperature of 25°C is represented by Equation (1). The GMWL is derived from global precipitation data, averaging numerous Local Meteoric Water Lines (LMWL), each with a different slope and intercept (Craig 1961).

$$\delta^2 H = 8\,\delta^{18}O + 10 \tag{1}$$

In this equation, all isotopic values ($\delta^{18}O$ and δ^2H) are expressed per mil (‰) on the VSMOW scale. The coefficient of 8 indicates that in rainwater samples, δ^2H is enriched by a factor of 8 more than $\delta^{18}O$. The intercept of 10 depends on climatic conditions, and this value changes under non-equilibrium conditions (Craig, 1961). The slope and the intercept of the line are influenced by secondary evaporation during precipitation. The isotopic composition of precipitation in different regions is close to the GMWL, and winter precipitation is much more depleted than summer precipitation.

Mixing

One of the common topics in groundwater studies is the investigation of groundwater composition, which may result from mixing two or more types of water. Examples include mixing surface water and groundwater between waters from an aquifer's upper and lower parts or waters from the recharge area and deep groundwater. The determination of mixing ratios depends on the complexity of the mixing process. Determining these ratios is relatively simple if mixing involves two types of water without adding or removing another phase, such as gases or minerals. However, if the mixing process involves three or more types of water, the mathematics of the problem becomes more complex (Hounslow, 2018).In this study, the following equation was used to calculate the contribution of each source to the groundwater recharge of the Evan Plain:

$$f_{AB} + f_{Ir} + f_D + f_{RK} = 1 \tag{2}$$

$$f_{AB}.\,cl_{AB} + f_{Ir}.\,cl_{Ir} + f_D.\,cl_D + f_{RK}.\,cl_{RK} = cl_{G.Ev}.\,100 \tag{3}$$

$$f_{AB}\left(\frac{cl}{Br}\right)_{AB} + f_{Ir}\left(\frac{cl}{Br}\right)_{Ir} + f_D\left(\frac{cl}{Br}\right)_D + f_{RK}\left(\frac{cl}{Br}\right)_{RK} = \left(\frac{cl}{Br}\right)_{G.Ev}.\,100 \tag{4}$$

$$f_{AB}(\delta18O)_{AB} + f_{Ir}(\delta18O)_{Ir} + f_D(\delta18O)_D + f_{RK}(\delta18O)_{RK} = (\delta18O)_{G.Ev}.\,100 \tag{5}$$

Where f_{AB}, f_{Ir}, f_D, f_{RK} represent each recharge source's contribution, including water from the Abbas Plain, the irrigation and drainage network, the Karkheh Reservoir Dam, and the Karkheh River. The parameters $cl_{G.Ev}$ و $(\delta18O)_{G.Ev}$ represent the concentration of chlorine and oxygen-18 in each well sampled in the Evan Plain.

Results and Discussion

Hydrogeology

Understanding the hydrogeological conditions of a region is critical for identifying the flow patterns and interactions within groundwater resources. An analysis of data from the exploitation wells in the Evan Plain revealed the presence of 279 operational wells scattered throughout the plain. These wells vary in depth across different parts of the region, with a general trend showing an increase in depth from an average of 11 meters in the east to 110 meters in the west. The total annual discharge from these wells is approximately 98 million cubic meters, with an average seasonal discharge of about 24 million. According to data from the Khuzestan Water and Power

Authority, there are 14 observation wells in the Evan Plain. The average groundwater level during the 2021-2022 water year was approximately 102.36 meters.

It is important to note that, since 2000, due to the construction of an irrigation and drainage network and extensive use of the Karkheh River, groundwater extraction through pumping from operational wells has decreased. As a result, the groundwater table has followed a relatively steady and upward trend since 2000, reducing the depth at which groundwater encounters the surface, making it more susceptible to surface contaminants and thereby increasing the potential for groundwater pollution.

A representative hydrograph is one of the most important tools for monitoring groundwater conditions in any aquifer. To this end, a hydrograph of the Evan Plain aquifer was plotted based on available data from the 2001-2002 to 2023-2024 water years (Fig. 3). As shown in the figure, groundwater levels have generally risen. While this increase reflects adequate aquifer recharge, improper management and failure to identify its recharge sources could lead to irreversible damages such as soil salinization. In this regard, a potentiometric map and flow direction map were also drawn (Fig. 4). As indicated in Figure 4, the general flow direction is from the north and northwest towards the south and southeast. The Karkheh River is a drainage channel for this plain, but in some parts of its course, it also recharges the plain. The groundwater depth map (Fig. 5) illustrates that groundwater levels are highest in the eastern and southeastern parts of the plain, where the ground surface is lower. In other words, in these areas, groundwater is closer to the surface (at depths of 5 to 15 meters from the ground).

All surrounding areas were evaluated after examining the flow mechanisms in the Evan Plain and determining the flow trends. Research conducted on the Abbas Plain, located west of the Evan Plain, showed that groundwater levels had risen since 2008, when irrigation and drainage operations began. The deepest groundwater is found in the eastern section, reaching depths of up to 50 meters, while the shallowest groundwater, at a depth of 1 meter, is located in the central part of the plain towards the west. To this end, flow direction and groundwater depth maps were drawn (Fig. 6 and Fig. 7). As shown in Figure 6, the flow direction in the Abbas Plain moves from the north and northwest towards the south and southeast, eventually reaching the Evan Plain. The elevation profile (AB) from the Abbas Plain to the Evan Plain indicates that the Abbas Plain is at a higher elevation than the Evan Plain (Fig. 8). Based on the flow direction map for the Abbas Plain, it is highly likely that water flows into the Evan Plain. Hydrochemical and isotopic sampling was conducted from both the Evan and Abbas plains to investigate this possibility further, and the results of these analyses are presented in the following sections.
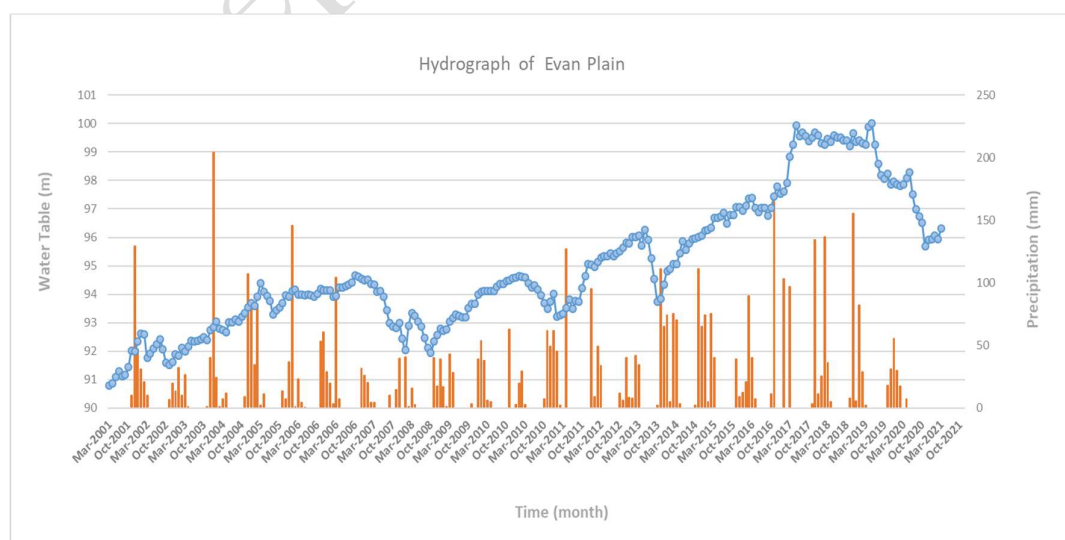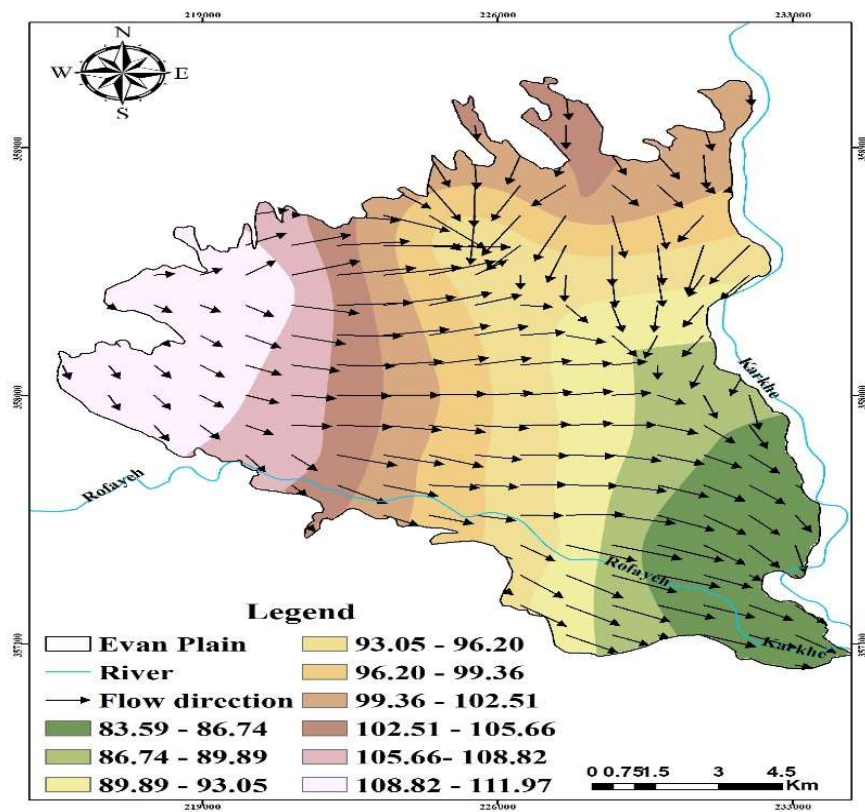

Figure 3. Hydrograph of the Evan Plain

Figure 4. Water table map and groundwater flow direction in the Evan Plain
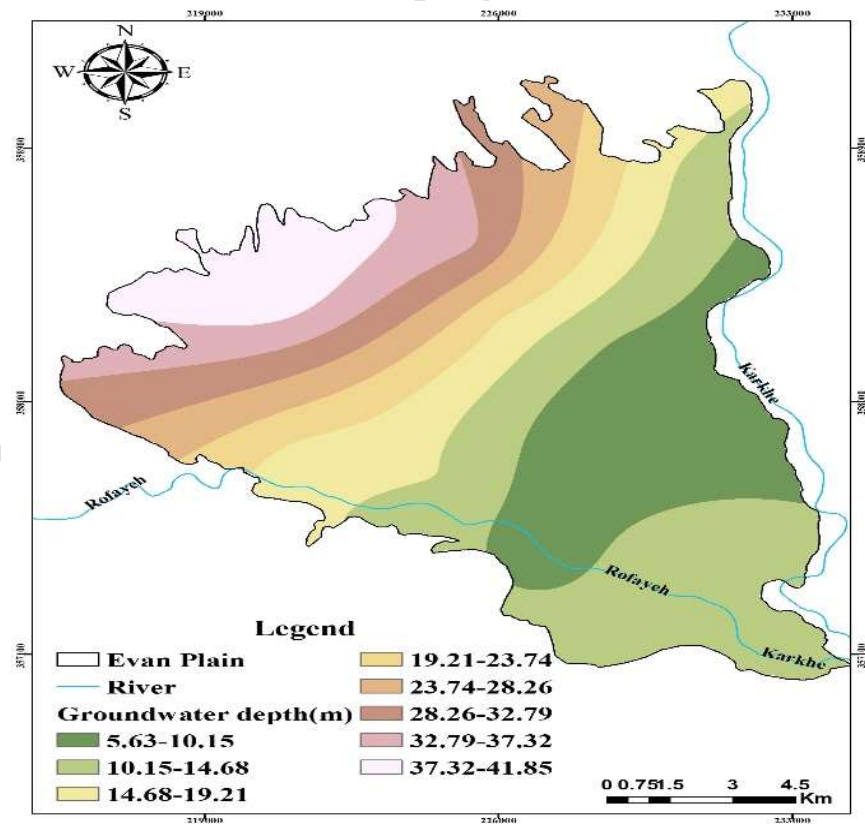

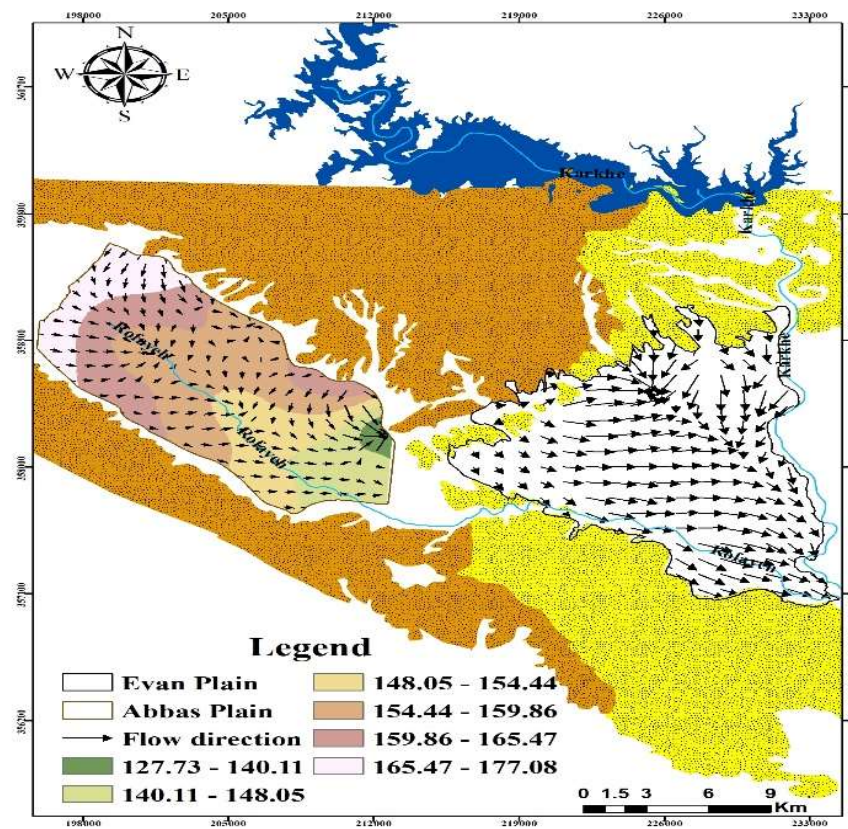**Figure 5.** Map of groundwater depth in the Evan Plain

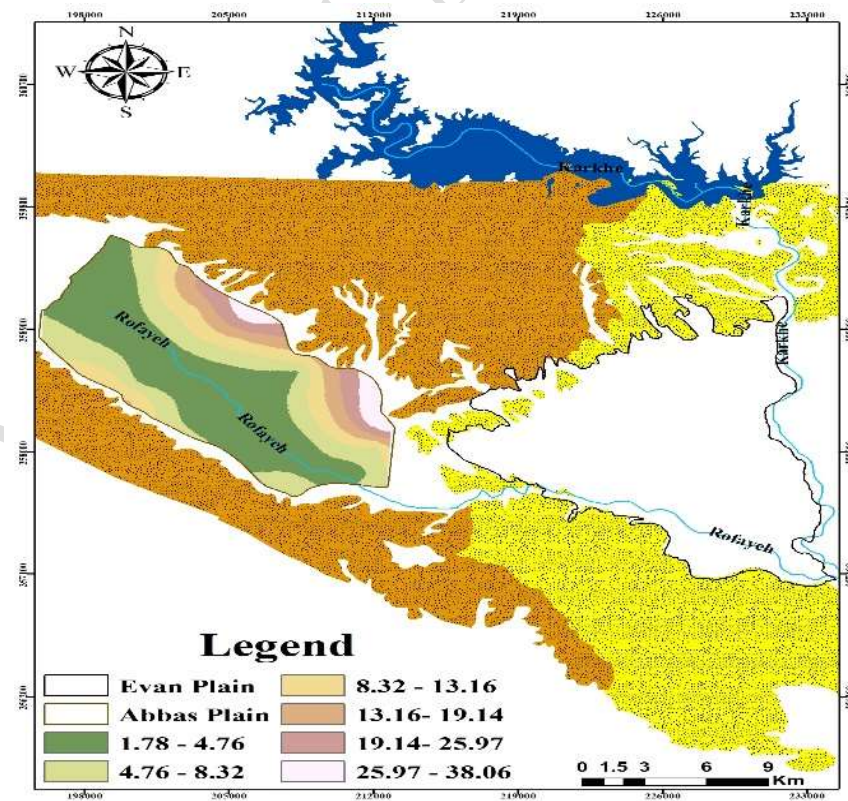**Figure 6.** Water table map and groundwater flow direction in the Abbas Plain

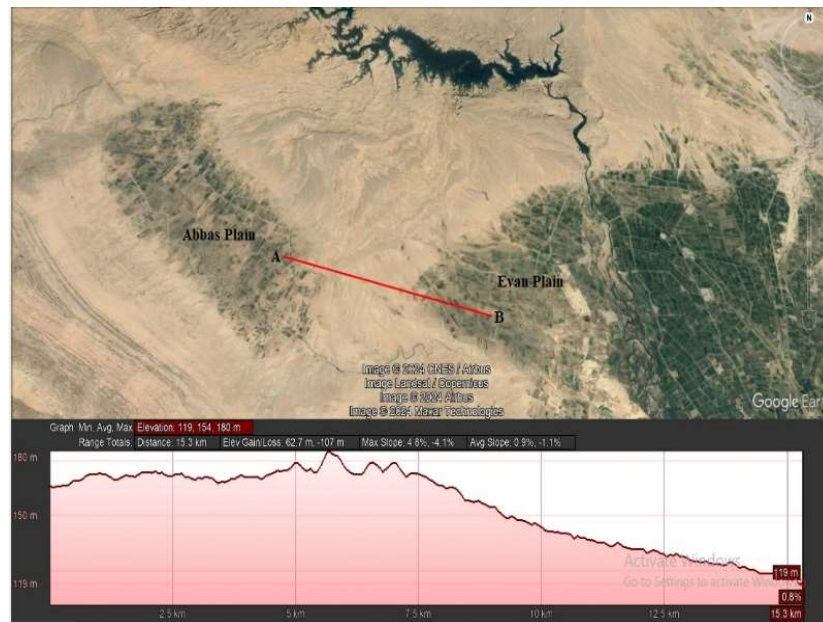**Figure 7.** Map of groundwater depth in the Abbas Plain

Figure 8. Elevation profile from Abbas Plain to Evan Plain

Hydrochemistry

One of the critical and determining factors in assessing and evaluating the quality of water resources is hydrochemical studies of the water sources in the region. Diagrams that allow simultaneous comparison of a large number of samples are used to analyze the results of hydrochemical analyses. One such diagram is the Piper diagram. The Piper diagram enables the simultaneous comparison of numerous samples and is employed to determine differences and similarities, as well as temporal and spatial changes in the types of water resources (Hounslow, 2018).

The results of the Piper diagram plotted for both the wet and dry periods indicate that the dominant groundwater types in the Evan Plain are magnesium sulfate and calcium sulfate. Additionally, the Piper diagram was used to assess the similarity and mixing of water resources from the samples taken from the Karkheh Dam (D), the Karkheh River (RK), the irrigation and drainage network (Ir), groundwater from Evan (EV), groundwater between the two plains of Evan and Abbas (BD), and groundwater from the Abbas Plain (AB) during both dry and wet periods (Fig. 9).

The results and the plotted Piper diagram show that the samples are grouped into two distinct clusters. According to this diagram, samples EV1, EV3, EV4, EV5, EV6, EV7, EV8, EV9, EV10, and EV11 are positioned close, indicating that they have a similar hydrochemical composition and originate from the same source. In the second group, groundwater samples EV12, EV13, EV14, EV15, EV16, EV17, EV18, EV20, EV21, and EV22 from the Evan Plain are positioned alongside groundwater samples from between the Evan and Abbas plains (BD1, BD2), as well as samples from the Abbas Plain (AB1, AB2, AB3, AB4). In this group, the samples from the irrigation and drainage network (Ir1, Ir2, Ir3, Ir4), the Karkheh River (RK1, RK2, RK3), and the Karkheh Dam (D1, D2) are also grouped.

As demonstrated in the hydrogeology section, the flow direction is from the Abbas Plain towards the Evan Plain, indicating that groundwater flows from the Abbas Plain into the Evan Plain. Figure 2 further confirms that the locations of these samples align along a single flow path. Additionally, based on the flow direction map of the Evan Plain (Fig. 4), the Karkheh River recharges the plain in certain areas. The influence of the Karkheh River's recharge effect is evident in the samples grouped in this cluster.
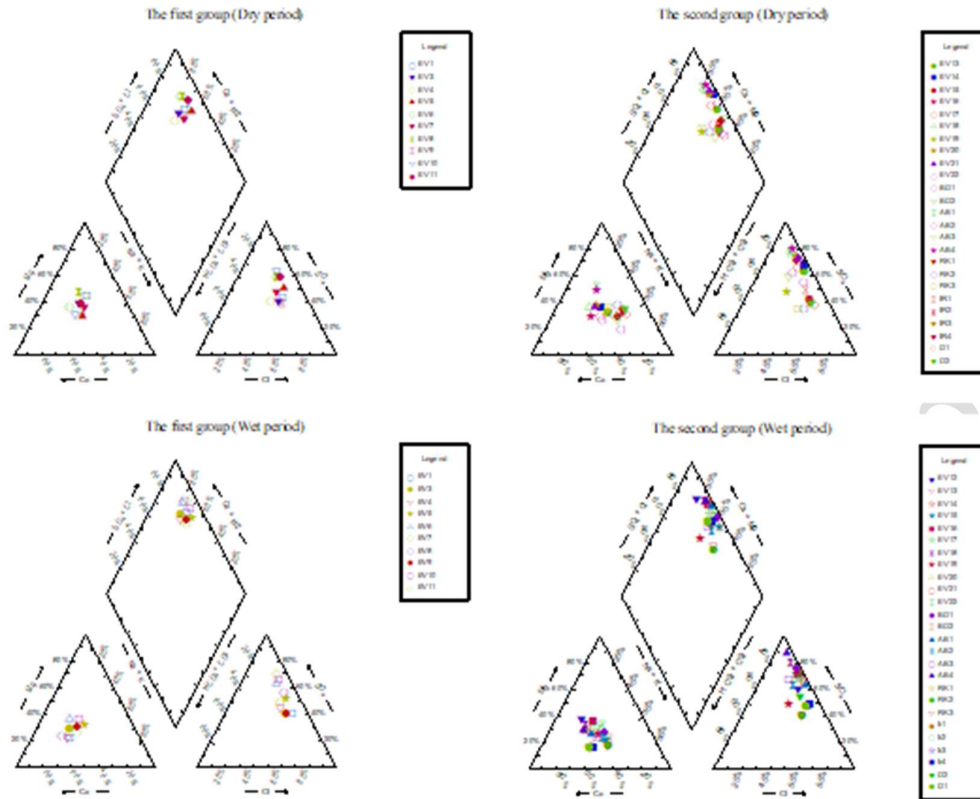
Figure 9. Piper diagram of the samples collected during the wet and dry seasons (2022-2023)

Hierarchical Cluster Analysis (HCA)

As explained in the methodology section, statistical clustering can be used to divide samples into distinct groups that are geologically and statistically significant (Steinhorst and Williams, 1985). HCA is the most common clustering method, providing intrinsic correlations between each sample and across all the data, typically displayed through a dendrogram. The dendrogram summarizes the clustering process, visualizes the clusters and their proximity, and significantly reduces the dimensions of the original data. The similarity (or linkage) between clusters and the separation of homogeneous clusters for the sampling locations are determined based on Euclidean distance.

As shown in Figure 10, the hierarchical cluster analysis, considering the hydrochemical parameters of groundwater samples from the Evan Plain Abbas Plain, as well as groundwater samples between the two plains, irrigation and drainage network samples from Evan Plain, and the river and Karkheh Dam samples, identified two clusters. This indicates that the Evan Plain has two distinct hydrochemical sources. In this case, samples EV2, EV4, EV8, EV11, EV9, EV3, EV6, EV7, EV10, EV5 and EV1 are grouped in cluster 1, while samples D1, EV21, RK3, Ir2, RK1, Ir1, Ir3, Ir4, RK2, EV22, EV18, EV20, EV19, EV17 and D2 are in sub-cluster 2-1, and samples AB1, EV16, BD1, EV13, EV14, AB4, BD2, EV15, AB3, EV12 and AB2 are in sub-cluster 2-2.

The location of samples in cluster 1, as shown on the spatial distribution map in Figure 3, indicates that these samples have similar hydrochemical compositions, suggesting that the samples in cluster 1 share a common origin. The samples grouped in cluster 2 suggest that the Karkheh River, the irrigation and drainage network, and the inflows from the Abbas Plain influence the groundwater in this part of the Evan Plain. Additionally, based on the spatial distribution map of the samples, it is evident that these samples are concentrated in a specific area.
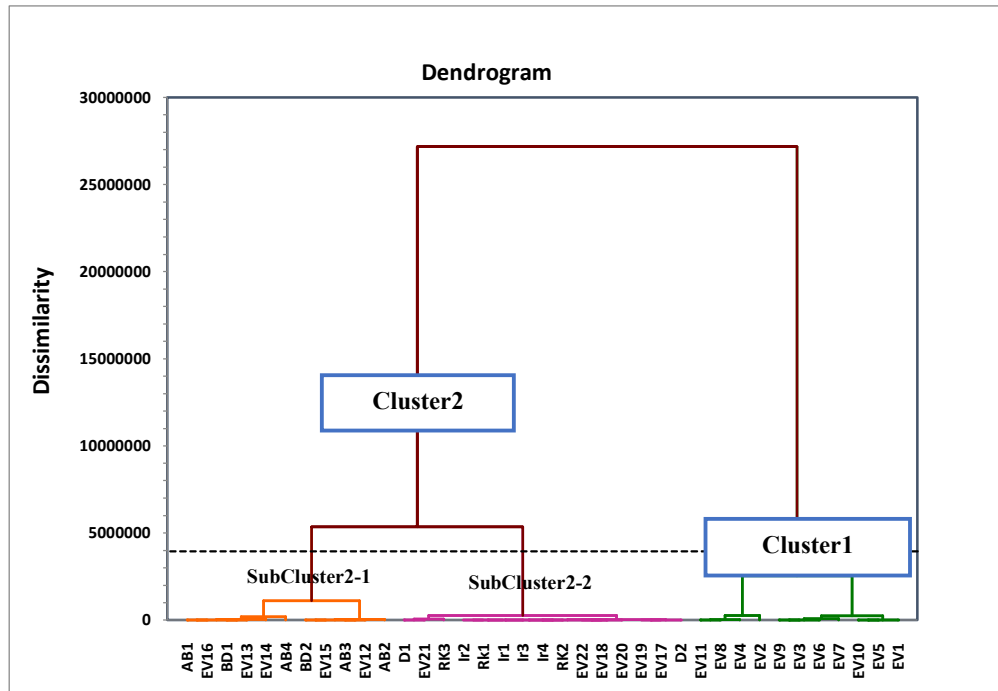
Figure 10. Dendrogram of groundwater samples from the Evan Plain, Abbas Plain, Karkheh River, and irrigation network

Isotopic Studies

As previously mentioned, one of the modern and precise methods for studying the origin of water sources is the use of stable isotopes of Oxygen-18 (^{18}O) and Deuterium (^{2}H) (Clark and Fritz, 1997).In the first step of isotopic analysis, the LMWL for the study area must be established. In other words, plotting the isotopic line of local precipitation is essential for any isotopic or hydrogeological study in the region. It is important to note that, until now, no research has plotted the LMWL for this region, and this study is the first to do so. Precipitation samples were collected in three different periods—December 2019, May 2022, and February 2023, to construct the LMWL for the Evan Plain. By plotting the isotopic content of the collected samples on the scatter plot of $\delta^{18}O$ versus $\delta^{2}H$, water sources were grouped into two categories (Fig. 11), with the distinction that during the dry season, due to more intensive evaporation, the sources exhibit a greater scatter.

The first group consists of some groundwater samples from the Evan Plain, which cluster around or close to the local meteoric isotopic line (Fig. 11). Therefore, the samples in this group are influenced by both evaporation and recharge from precipitation. The placement of these samples within a specific range also indicates their common origin. The second group includes other groundwater samples from the Evan Plain, the Abbas Plain, the Karkheh River, the irrigation and drainage network, and the Karkheh Dam. The clustering of these samples suggests that mixing has occurred, and they share a common origin.

Calculation of Contribution from Recharge Sources

contribution of each recharge source for each sampled well in the Evan Plain was calculated (Table 3) using equations 2 to 5. The results indicate that in wells from group 1, the contribution of recharge from the Karkheh River ranges from 22.72% to 38.51%, with an average of 30.09%, indicating it has the greatest influence in these areas. In group 2, the recharge contribution from

the Abbas Plain varies between 28.31% and 37.08%, with an average of 31.62%, demonstrating that it plays the most significant role in this group (Fig. 12).

According to the calculations for determining the contribution of each recharge source, it was found that the Karkheh River provides the highest recharge contribution in group 1 wells (EV1, EV2, EV3, EV4, EV5, EV6, EV7, EV8, EV9, EV10, EV11), which, as indicated by the flow direction map of the Evan Plain (Fig. 4), shows that the river recharge the plain in these areas. In group 2 wells (EV12, EV13, EV14, EV15, EV16, EV17, EV18, EV19, EV20, EV21, EV22), the inflows from the Abbas Plain and Karkheh Dam have the most significant recharge role, which is consistent with the flow direction maps of both the Evan and Abbas Plains (Fig. 4 and Fig.5), indicating that the flow moves from the Abbas Plain toward the Evan Plain.
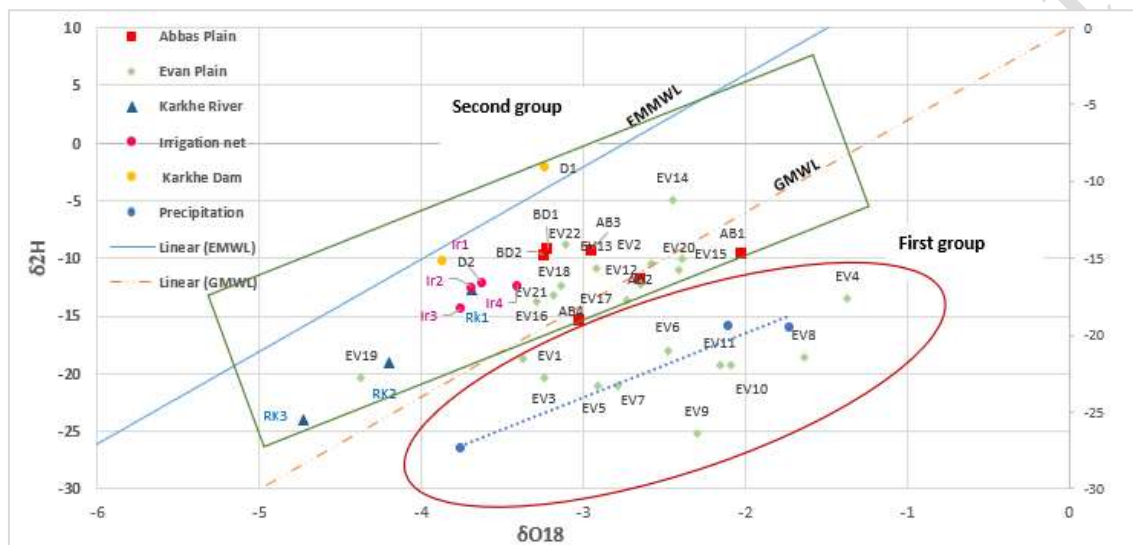

Figure 11. Distribution of samples on the δ¹⁸O vs δ²H plot

Table 3. Results derived from the assessment of recharge source contributions in the Evan Plain

| Sample Name	Abbas Plain (%)	Irrigation net (%)	Dam (%)	Karkhe River (%)
EV1	21.09	25.42	22.77	30.72
EV2	20.02	27.71	20.80	31.48
EV3	20.55	26.56	21.78	31.10
EV4	31.85	2.49	42.48	23.17
EV5	16.20	32.41	13.95	37.43
EV6	21.33	24.91	23.20	30.56
EV7	16.93	31.53	15.26	36.28
EV8	30.53	5.31	40.06	24.10
EV9	18.86	23.69	18.94	38.51
EV10	29.22	8.10	37.66	25.02
EV11	30.04	8.14	39.09	22.72
EV12	33.44	10.31	44.94	11.31
EV13	31.92	12.22	36.46	19.41
EV14	28.32	14.84	33.43	23.41
EV15	37.09	1.40	45.80	15.71
EV16	29.76	15.02	33.62	21.60
EV17	31.39	27.43	21.03	20.14
EV18	31.14	26.68	21.68	20.50
EV19	33.75	34.58	14.88	16.79
EV20	28.71	28.03	19.30	23.96
EV21	31.16	26.74	21.62	20.47
EV22	31.21	26.88	21.51	20.40
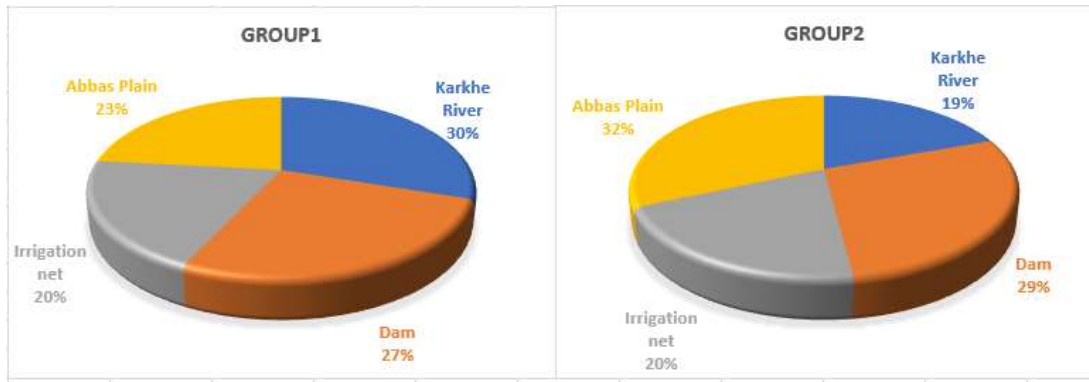
Figure 12. Distribution Percentage of Recharge Sources for Wells in Groups 1 and 2

Conclusion

The hydrograph of the Evan Plain aquifer from the 2001-2002 to the 2023-2024 water year indicates an increasing trend in the groundwater level of the region. Since 2000, groundwater extraction from operational wells has decreased due to the construction of the irrigation and drainage network and the utilization of water from the Karkheh River. As a result, the aquifer level has risen since 2000, reducing the depth of the unsaturated zone and increasing the potential for groundwater contamination in the region.

According to the flow direction map, the general flow direction is from the north and northwest toward the south and southeast. The Karkheh River acts primarily as a drain for the plain along most of its course, but it also recharges the plain in some sections. The groundwater depth map shows that the groundwater table is higher in the eastern and southeastern parts of the plain, with groundwater being closer to the surface in these areas (5 to 15 meters from the surface) than other parts of the plain. The flow direction map also reveals that inflows to the plain from the northwest and southwest are related to the Abbas Plain.

The results of hydrochemical analyses show that the samples are divided into two distinct groups. The first group corresponds to groundwater sources located in the northern and northeastern parts of the Evan Plain. The second group includes groundwater samples from the plain's central, southeastern, and southwestern parts. The samples in this second group cluster with groundwater samples from the Abbas Plain, groundwater samples between the two plains (Evan and Abbas), the Karkheh River, the irrigation and drainage network, and the sample from the Karkheh Dam, indicating a common origin and mixing of these water sources.

HCA, based on the hydrochemical parameters of groundwater samples from the Evan Plain, the Abbas Plain, and the samples between the two plains, as well as samples from the irrigation and drainage network, the Karkheh River, and the Karkheh Dam, grouped the samples into two clusters that suggests that the water sources in the Evan Plain have two distinct hydrochemical origins.

Isotopic studies, illustrated by the $\delta^{18}O$ versus δ^2H plot, further revealed two groups of samples. The first group consists of some groundwater samples from the Evan Plain, which are located around or close to the LMWL, indicating that they are primarily influenced by evaporation and recharge from precipitation. The second group includes groundwater samples from the Abbas Plain, the Karkheh River, the irrigation and drainage network, and the sample from the Karkheh Dam, with their close grouping suggesting a common origin.

Overall, the findings indicate that the Karkheh River, the irrigation and drainage network, the Karkheh Dam, and inflows from the Abbas Plain are the primary recharge sources for the Evan Plain. The results also show that in group 1 wells, the Karkheh River provides the highest recharge contribution, with an average of 30.09%. In group 2, the Abbas Plain contributes the most, averaging 31.62 (Fig. 9).

Limitations and Future Research Directions

While this study provides valuable insights into groundwater recharge mechanisms in the Evan Plain, it is important to acknowledge its limitations. Spatial variability in recharge sources was assessed using data from a limited number of sampling locations, which may not capture the full complexity of the aquifer system. Additionally, isotopic analyses were limited to the dry season, and therefore, seasonal variations in recharge dynamics inferred from isotopic data remain unexplored. Methodologically, uncertainties inherent in isotopic and hydrochemical mixing models may influence the precision of recharge source estimates.

Future studies should address these limitations by conducting isotopic sampling campaigns across different seasons and expanding the spatial coverage to adjacent aquifer systems. Advanced isotopic techniques, such as radiocarbon dating, could provide a more refined understanding of recharge timescales. Integrating hydrochemical and isotopic results with numerical groundwater models would enhance predictions of recharge dynamics and their sensitivity to environmental changes. Establishing long-term monitoring programs will ensure consistent data collection and support sustainable groundwater management strategies in the region.

Conflicts of interest or competing interests

The authors have no relevant financial or non-financial interests to disclose.

Ethics approval and consent to participate: Not applicable

Consent for publication: Not applicable

Availability of data and materials: The datasets used and/or analyzed during the current study are available from the corresponding author on reasonable request.

Declaration of Generative AI and AI-assisted technologies in the writing process

The authors declare that no generative AI or AI-assisted technologies were used in the writing process.

Authors' contributions

All authors (Zahra Chaghazardi, Seyed Yahya Mirzaee, Manouchehr Chitsazan, Farshad Alijani) have an equal share in writing all parts of the article.

References

Al-Ruwaili, S., Alharbi, H. A., Alsharif, W., 2023. Identifying groundwater recharge sources using

stable isotopes and multivariate analysis in the Wadi Qanun Basin, Saudi Arabia. Sustainability, 15(3): 2401.

Balagizi, C. M., 2022. Characterizing groundwater recharge sources using water stable isotopes in the North Basin of Lake Kivu, East Africa. Chemical Geology 594: 120778.

Belkhiri, L., 2011. A multivariate statistical analysis of groundwater chemistry data.

Bouimouass, H., 2020. Groundwater recharge sources in semiarid irrigated mountain fronts. Hydrological Processes 34(7): 1598-1615.

Chitsazan, M., 2018. Evaluation of Groundwater Nitrate Pollution Based on Main Components and Factor Analysis (Case Study: Karaj Plain Aquifer). Iranian Journal of Ecohydrology 5(4): 1119-1133.

Clark, I. D., P. Fritz .,1997. Environmental Isotopes in Hydrogeology, Taylor & Francis.

Cocca, D., 2024. Assessment of the groundwater recharge processes of a shallow and deep aquifer system (Maggiore Valley, Northwest Italy): a hydrogeochemical and isotopic approach. Hydrogeology Journal 32(2): 395-416.

Craig, H., 1961. Isotopic variations in meteoric waters .Science 133(3465): 1702-1703.

Dar, F. A., et al., 2021. Groundwater recharge in semiarid karst context using chloride and stable water isotopes. Groundwater for Sustainable Development 14: 100634.

Davis, J. C. and R. J. Sampson.,1986. Statistics and data analysis in geology, Wiley New York.

Fu, C., et al., 2018. A hydrochemistry and multi-isotopic study of groundwater origin and hydrochemical evolution in the middle reaches of the Kuye River basin. Applied Geochemistry 98: 82-93.

Gat, J., 2010. Isotope hydrology: a study of the water cycle, World Scientific.

Gleeson, T., 2016. The global volume and distribution of modern groundwater. Nature Geoscience 9(2): 161-167.

Hounslow, A., 2018. Water quality data: analysis and interpretation, CRC press.

Huang, X., 2021. A study on groundwater recharge in the Anyanghe River alluvial fan, North China Plain, based on hydrochemistry, stable isotopes and tritium. Hydrogeology Journal 29(6).

Joshi, S. K., et al., 2018. Tracing groundwater recharge sources in the northwestern Indian alluvial aquifer using water isotopes (δ18O, δ2H and 3H). Journal of Hydrology 559: 835-847.

Karlović, I., 2021. Groundwater recharge assessment using multi-component analysis: Case study at the NW edge of the Varaždin Alluvial Aquifer, Croatia. Water 14(1): 42.

Klantari, N., 2012. The qualitative effect of Karkheh dam on Avan plain aquifer in Dezful in Khuzestan province. Iran-Water Resources Research 8(1): 1-9.

Kumar, C., 2012. Climate change and its impact on groundwater resources. International Journal of Engineering and Science 1(5): 43-60.

Marques, J. M., 2013. Isotopic and hydrochemical data as indicators of recharge areas, flow paths, and water-rock interaction in the Caldas da Rainha–Quinta das Janelas thermomineral carbonate rock aquifer (Central Portugal). Journal of Hydrology 476: 302-313.

Mirzaee, S. Y., 2019. Determination of the hydraulic Connection between the Ḳīno anticline springs (Khuzestan province) using hydrochemical data, principal component analysis (PCA), and hierarchical cluster (HCA). Advanced Applied Geology 9(2): 133-141.

Mohammadzadeh, H. and E. Eskandari., 2018. Application of hydrologeochemical and isotopic techniques for better understanding of water resources characteristics in Paveh and Javanrud study areas, Kermanshah. Hydrogeology 3(1): 80-98

Moussa, A., Favreau, G., Nazoumou, Y., 2024. Groundwater recharge processes in the Lake Chad Basin using isotopic and hydrochemical tracers. Hydrogeology Journal, 32(1), 77–91.

Nakić, Z., 2013. Conceptual model for groundwater status and risk assessment-case study of the Zagreb aquifer system. Geologia Croatica 66(1): 55-76.

Parlov, J., 2019. Using water stable isotopes for identifying groundwater recharge sources of the unconfined alluvial Zagreb aquifer (Croatia). Water 11(10): 2177.

Parlov, J., 2012. Origin and dynamics of aquifer recharge in Zagreb area. International Conference on water, climate, and environment, Balwois.

Putra, A. R., Fathurrahman, F., 2024. Identification of recharge zones in a multilayer volcanic aquifer using hydrochemical and isotopic approaches. Hydrogeology Journal, 32(2): 201-217.

Schwarz, K., 2009. Mixing and transport of water in a karst catchment: a case study from precipitation via seepage to the spring. Hydrology and Earth System Sciences 13(3): 285-292.

Shrestha, S., F. Kazama., 2007. Assessment of surface water quality using multivariate statistical techniques :A case study of the Fuji river basin, Japan. Environmental Modelling & Software 22(4): 464-475.

Steinhorst, R. K. and R. E. Williams., 1985. Discrimination of groundwater sources using cluster analysis, MANOVA, canonical analysis and discriminant analysis. Water Resources Research 21(8): 1149-1156.

Wada, Y., 2012. Nonsustainable groundwater sustaining irrigation: A global assessment. Water Resources Research 48(6).

Wang, L., 2015. Using hydrochemical and isotopic data to determine sources of recharge and groundwater evolution in an arid region: a case study in the upper–middle reaches of the Shule River basin, northwestern China. Environmental Earth Sciences 73: 1901-1915.

Xu, F., 2023. Integration of hydrochemistry and stable isotopes for assessing groundwater recharge and evaporation in pre-and post-rainy seasons in Hua County, China. Natural Resources Research 32(5): 1959-1973.